First Synthesis, Experimental and Theoretical Vibrational Spectra of an Oxametallacycle on a Metal Surface

G. Scott Jones,[†] Manos Mavrikakis,[†] Mark A. Barteau,*[,†] and John M. Vohs[‡]

Contribution from the Center for Catalytic Science and Technology, Department of Chemical Engineering, University of Delaware, Newark, Delaware 19716, and Department of Chemical Engineering, University of Pennsylvania, Philadelphia, Pennsylvania 19104

Received October 16, 1997

Abstract: High-resolution electron energy loss spectroscopy (HREELS) studies were performed to examine the reactions of 2-iodoethanol (ICH_2CH_2OH) on the Ag(110) surface. The goal of these experiments was to isolate and spectroscopically characterize a stable surface oxametallacycle, an intermediate previously proposed but never isolated in the chemistry of a variety of oxygenates, including epoxides. The hydroxyethyl intermediate ($-CH_2CH_2OH$), formed from initial carbon−iodine bond scission, decomposed at 263 K to yield a variety of volatile products as well as a surface oxametallacycle ($-CH_2CH_2O-$). The oxametallacycle intermediate, formed at 263 K, remained intact until 340 K, permitting spectroscopic characterization by HREELS. Density Functional Theory (DFT) calculations were employed to determine the fully optimized structure for the oxametallacycle on silver and to predict the infrared spectrum and molecular motions for that structure. The excellent agreement between the infrared spectrum predicted for an oxametallacycle incorporating two silver atoms and the experimental HREEL spectrum conclusively identifies the surface oxametallacycle. The principal reaction channel for this intermediate in temperature programmed desorption (TPD) experiments is coupling of two oxametallacycles to form the cyclic product γ-butyrolactone, rather than the anticipated ring closure pathway to form ethylene oxide. However, one of the vibrational modes predicted by DFT appears to be a possible reaction coordinate for the conversion of oxametallacycles to ethylene oxide.

Introduction

Considerable effort has been devoted worldwide over the last fifteen years to improving the selectivity of the silver-catalyzed epoxidation of ethylene with dioxygen,[1] to extending this catalysis to other olefins and diolefins,[2] and to developing homogeneous catalysts for olefin epoxidation.[3−6] The desirability of high-value-added epoxide and glycol products of these reactions and the lack of success in extrapolating the silver-catalyzed epoxidation of ethylene to higher olefins continue to drive considerable efforts in catalytic olefin epoxidation, both homogeneous and heterogeneous. Although many advances have been made in the understanding of ethylene epoxidation, the exact mechanism, including intermediates or transition states, remains unresolved.

Surface oxametallacycles and their single metal atom analogues in homogeneous media, metallaoxetanes, are typically depicted with the structures shown below. Metallaoxetanes have

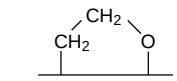

surface oxametallacycle

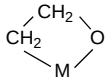

metallaoxetane

been proposed as crucial intermediates in a variety of homogeneously catalyzed reactions, including selective olefin oxidation, asymmetric dihydroxylation and epoxidation processes, carbonylation and decarbonylation chemistry, insertion of other unsaturated functions, and metathetical reactions.[7] Likewise surface oxametallacycles have been implicated in olefin oxidation, alcohol decarbonylation, and epoxide synthesis and decomposition. Of particular interest is the suggested role of metallaoxetanes and oxametallacycles in the chemistry of epoxides.

Despite previous indications that oxametallacycles are intermediates in the chemistry of epoxides on transition metal surfaces, the sole extant examples of the isolation of such complexes are in homogeneous media, e.g., as organometallic complexes in solution and in matrix isolation experiments trapping gaseous species. These homogeneous examples of metallaoxetane synthesis often involve ring-opening or ring-forming reactions of epoxides as well. For example, Margrave and co-workers have spectroscopically characterized metallaoxetanes formed by insertion of either Fe[8] or Ni[9] atoms into the carbon−oxygen bond of ethylene oxide in an argon matrix. Graziani et al. have used three-dimensional X-ray diffraction to identify the platinaoxetanes formed from the ring opening of tetra- and tricyano-substituted ethylene oxide in solution.[10,11] In addition, metallaoxetanes have been proposed as intermediates in olefin epoxidation reactions catalyzed by Cr complexes in solution.[12] This suggestion is further supported by theoretical

* To whom correspondence should be addressed.
[†] University of Delaware.
[‡] University of Pennsylvania.

(1) van Santen, R. A.; Kuipers, H. P. C. E. *Adv. Catal.* **1987**, *35*, 265.
(2) Monnier J. R. Presented at the *Third World Congress on Oxidation Catalysis*, San Diego, CA, 1997.
(3) Clerici, M. G.; Ingallina, P. *J. Catal.* **1993**, *140*, 71.
(4) Hutter, R.; Mallat, T.; Baiker, A. *J. Catal.* **1995**, *153*, 177.
(5) Tokunaga, M.; Larrow, J. F.; Kakiuchi, F.; Jacobsen, E. N. *Science* **1997**, *277*, 936.
(6) Rudolph, J.; Reddy, K. L.; Chiang, J. P.; Sharpless, K. B. *J. Am. Chem. Soc.* **1997**, *119*, 6189.
(7) Jorgensen, K. A.; Schiott, B. *Chem. Rev.* **1990**, *90*, 1483.
(8) Kafafi, Z. H.; Billups, W. E.; Hauge, R. H.; J. L. Margrave, *J. Am. Chem. Soc.* **1987**, *109*, 4775.
(9) Kline, E. S.; Margrave, J. L.; Hauge, R. H.; Kafafi, Z. H. *High-Temp. Sci.* **1991**, *30*, 69.

S0002-7863(97)03609-3 CCC: $15.00
Published on Web 03/24/1998

studies performed by Rappé and Goddard which show that the formation of the chromaoxetane is likely.[13]

There are clear parallels between the chemistry of metallaoxetanes in solution and the reactions attributed to surface oxametallacycles. Indeed, the same reactions described above as leading to metallaoxetane formation also have been proposed to yield oxametallacycles on extended metal surfaces. Epoxide ring opening to form oxametallacycles has been suggested to take place on a number of Group VIII metal surfaces, including Pd(110),[14] Pd(111),[15] and Rh(111).[16] Friends and co-workers have demonstrated oxygen addition to olefins on Rh(111)−(2×1)O[17−19] and have performed extended Hückel calculations in support of the proposed oxametallacycle intermediates formed by this reaction.[20] Finally, an additional route to oxametallacycles proposed on metal surfaces involves hydride elimination from surface alkoxides; examples include the reactions of *tert*-butoxide on Ag(110)[21,22] and of various C_2-C_4 aliphatic alcohols on Rh(111).[23−29] In the former case the principal volatile product observed is isobutylene oxide, thus providing a link between surface oxametallacycles and epoxide formation.

The limited studies to date have invoked surface oxametallacyles in order to explain product formation channels observed in TPD experiments; these intermediates have *not* previously been observed directly. An essential part of understanding surface oxametallacycle reactions, and of manipulating the selectivity of these to produce desirable products such as epoxides, is therefore to isolate stable examples which can be probed by spectroscopic and chemical methods. We report here the first example of a stable oxametallacycle on a metal surface. The synthesis on Ag(110) involves scission of the C−I bond of 2-iodoethanol, $I-CH_2CH_2OH$, to produce hydroxyethyl, $-CH_2-CH_2OH$; dehydrogenation of this intermediate generates the oxametallacycle. Presented below are the first vibrational spectra of a surface oxametallacycle along with mode assignments determined by means of Density Functional Theory (DFT) calculations.

Experimental Section

All experiments were performed in either of two ultrahigh vacuum (UHV) chambers. Temperature-programmed desorption (TPD) experiments were carried out in a modified Physical Electronics Model 548 surface analysis system. The details of those TPD experiments have been described elsewhere.[30] High-resolution electron energy loss spectroscopy (HREELS) experiments were performed in a separate UHV chamber with a base pressure of 1×10^{-10} Torr. The chamber was equipped with an LK Technologies ELS 3000 spectrometer, the design of which has been extensively described by Ibach.[31] All of the spectra were collected in the specular direction with the electron beam incident 60° from the surface normal. The HREELS experiments were conducted at an electron beam energy of 3 eV and a full width at half-maximum (fwhm) resolution of 24−30 cm^{-1} for the elastically scattered beam.

The silver single crystal was aligned to the (110) orientation by the Laue method, cut, and mechanically polished by using standard metallographic techniques. Initial cleaning of the Ag(110) crystal was achieved by cycles of argon ion bombardment followed by annealing at 1000 K. Any residual carbon left on the surface was desorbed in the form of CO_2 by successive cycles of oxygen exposure and TPD. The surface cleanliness was tested by using HREELS and oxygen-TPD while the sample orientation was verified by using low-energy electron diffraction (LEED).

The two UHV chambers used in this work had dissimilar dosing arrangements for introducing 2-iodoethanol to the Ag(110) crystal. In the TPD experiments, the sample was placed approximately 1 cm from a stainless steel capillary which was used to directly dose 2-iodoethanol. Variations in exposure were accomplished by altering the pressure in the dosing manifold and/or changing the duration of the dose. The HREELS chamber was not equipped for direct dosing. The 2-iodoethanol doses in the HREELS experiments were therefore accomplished by backfilling the UHV chamber with 2-iodoethanol and monitoring the dosing time at a given pressure. The doses were recorded in langmuirs (L), where 1 L = 10^{-6} Torr·s. The 2-iodoethanol used in both sets of experiments (99%, Aldrich) was purified by repeated freeze−pump−thaw cycles.

Computational Details

The Amsterdam Density Functional (ADF) program was implemented to calculate the fully optimized structure for an oxametallacycle adsorbed onto a flexible silver dimer. The fully optimized structure found corresponds to the geometry representing the minimum total energy. More details on calculations yielding the optimal structure can be found elsewhere.[32] Following the geometry optimization of the oxametallacycle, ADF was used to predict the infrared spectrum of the fully optimized oxametallacycle. Linear combinations of atomic Slater-type orbitals are employed by ADF to represent the molecular orbitals, and the Kohn−Sham one-electron equations are solved self-consistently. The local spin-density exchange-correlation potential is represented by the Vosko−Wilk−Nusair (VWN) functional.[33] Gradient corrections for the exchange and correlation energy terms were included self-consistently by using the functionals developed by Becke[34] and Perdew,[35] respectively. The basis sets employed in the calculations were of double-ζ quality, and relativistic effects were neglected. Two-point frequency calculations with an integration accuracy of 10^{-6} were performed on the fully optimized oxametallacycle structure by using the same functionals as those described above.

Results

The results presented herein are separated into three sections. The first section describes the temperature-programmed desorption of 2-iodoethanol (IEtOH) on the clean Ag(110) surface under ultrahigh vacuum conditions. These TPD experiments have been reported previously[30] and are only briefly summarized here. The second section describes the interpretation of the HREEL spectra for the surface intermediates involved in that chemistry. The final section reports the results of Density

(10) Lenarda, M.; Calligaris, M.; Pahor, N. B.; Graziani, M.; Randaccio, L. *J. Chem. Soc., Dalton Trans.* **1978**, 279.
(11) Schlodder, R.; Lenarda, M.; Ibers, J. A.; Graziani, M. *J. Am. Chem. Soc.* **1974**, *96*, 6893.
(12) Sharpless, K. B.; Backvall, J. E.; Teranashi, A. Y. *J. Am. Chem. Soc.* **1977**, *99*, 3120.
(13) Rappé, A. K.; Goddard, W. A., III *J. Am. Chem. Soc.* **1982**, *104*, 3287.
(14) Shekhar, R.; Barteau, M. A. *Surf. Sci.* **1996**, *348*, 55.
(15) Lambert, R. M.; Ormerod, R. M. *Langmuir* **1994**, *10*, 730.
(16) Brown, N. F.; Barteau, M. A. *Surf. Sci.* **1993**, *298*, 6.
(17) Xu, X.; Friend, C. M. *J. Am. Chem. Soc.* **1991**, *113*, 6779.
(18) Xu, X.; Friend, C. M. *J. Phys. Chem.* **1991**, *95*, 10753.
(19) Xu, X.; Friend, C. M. *J. Am. Chem. Soc.* **1990**, *112*, 4571.
(20) Calhorda, M. J.; Friend, C. M.; Lopes, P. E. M. *J. Mol. Catal. A* **1995**, *97*, 157.
(21) Brainard, R. L.; Madix, R. J. *J. Am. Chem. Soc.* **1987,** *109*, 8082.
(22) Brainard, R. L.; Madix, R. J. *J. Am. Chem. Soc.* **1989**, *111*, 3826.
(23) Houtman, C. J.; Barteau, M. A. *J. Catal.* **1991,** *130*, 528.
(24) Brown, N. F.; Barteau, M. A. *Langmuir* **1992**, *8*, 862.
(25) Brown, N. F.; Barteau, M. A. *J. Am. Chem. Soc.* **1992**, *114*, 4258.
(26) Brown, N. F.; Barteau, M. A. in *Selectivity in Catalysis*; Davis, M. E., Suib, S. L., Eds.; ACS Symp. Ser. No. 517; American Chemical Society: Washington, DC, 1993; p 345.
(27) Brown, N. F.; Barteau, M. A. *J. Phys. Chem.* **1994**, *98*, 12737.
(28) Brown, N. F.; Barteau, M. A. *Langmuir* **1995**, *11*, 1184.
(29) Brown, N. F.; Barteau, M. A. *J. Phys. Chem.* **1996**, *100*, 2269.
(30) Jones, G. S.; Barteau, M. A. *J. Vac. Sci. Technol. A* **1997**, *15*, 1667.
(31) Ibach, H. *Electron Energy Loss Spectrometer;* Hawkes, P. W., Ed.; Springer Series in Optical Sciences, No. 63; Springer-Verlag: Berlin, 1991.
(32) Mavrikakis, M.; Doren, D. J.; Barteau, M. A. *J. Phys. Chem. B* **1998**, *102*, 394
(33) Vosko, S. H.; Nusair, M.; Wilk, L. *Can. J. Phys.* **1980**, *58*, 1200.
(34) Becke, A. D. *Phys. Rev. A* **1988**, *38*, 3098.
(35) Perdew, J. P. *Phys. Rev. B* **1986**, *33*, 8822.

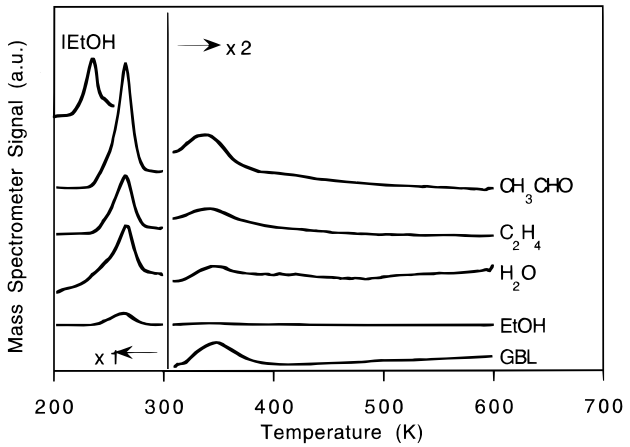

Figure 1. TPD spectra following a saturation dose of 2-iodoethanol on Ag(110). GBL = γ-butyrolactone.

Table 1. Yields (ML) of Volatile Products Evolved at 263 and 340 K for Saturation Exposure of 2-Iodoethanol on Ag(110) at 200 K

products	263 K	340 K
H_2O	0.087	0.019
C_2H_4	0.093	0.020
CH_3CHO	0.180	0.052
C_2H_5OH	0.018	0.001
γ-butyrolactone (GBL)	0.000	0.028
overall stoichiometry	$C_2H_{4.8}O_{0.98}$	$C_2H_{3.9}O_{0.99}$

Functional Theory calculations which are used to assign the modes of the experimentally obtained HREEL spectra.

Temperature-Programmed Reaction Studies. Unlike simple alcohols, which require the presence of adsorbed oxygen in order to undergo reaction on silver surfaces,[36,37] 2-iodoethanol (IEtOH) readily reacts on the clean Ag(110) surface. The TPD spectra of the products evolved after a saturation exposure of IEtOH on the clean Ag(110) surface are shown in Figure 1. By using previously described methods,[30] the saturation coverage for reacting IEtOH was determined to be 0.42 monolayers, where a monolayer is defined as the number of silver atoms contained on the ridges of the ideal Ag(110) surface (8.4×10^{14} atoms/cm^2). Molecular IEtOH desorbed from the Ag(110) surface at 225 K. The reacting 0.42 monolayers of IEtOH decomposed via either of two reaction channels at 263 K and 340 K, both of which produced acetaldehyde, ethylene, ethanol, and water. In addition to C_2 products, the 340 K reaction channel also produced a cyclic ester, γ-butyrolactone (GBL), which accounted for the largest fraction of carbon-containing products evolved at this temperature. To our knowledge γ-butyrolactone (GBL) has not previously been synthesized by surface reactions under UHV conditions. The absolute yields of the products desorbing at 263 K and 340 K are listed in Table 1 in terms of monolayers. A thorough discussion of the deconvolution of the TPD spectra is included in our previous report.[30]

The 263 K reaction channel has an overall volatile product stoichiometry of $C_2H_{4.8}O_{0.98}$, i.e., C_2H_5O, which is consistent with its assignment as either an ethoxide ($-OCH_2CH_3$) or a hydroxyethyl ($-CH_2CH_2OH$) species. However, ethoxides formed in separate experiments by reaction of ethanol with an oxygen-precovered Ag(110) surface decomposed at 294 K,[38] suggesting that the 263 K intermediate is not an ethoxide. In addition, the 263 K reaction channel produced ethylene and water in a 1:1 ratio whereas no ethylene formation was observed for ethoxide decomposition.[36] Therefore we have proposed that the surface species which decomposes at 263 K is a hydroxyethyl intermediate ($-CH_2CH_2OH$) formed by carbon−iodine scission of the IEtOH reactant.[30]

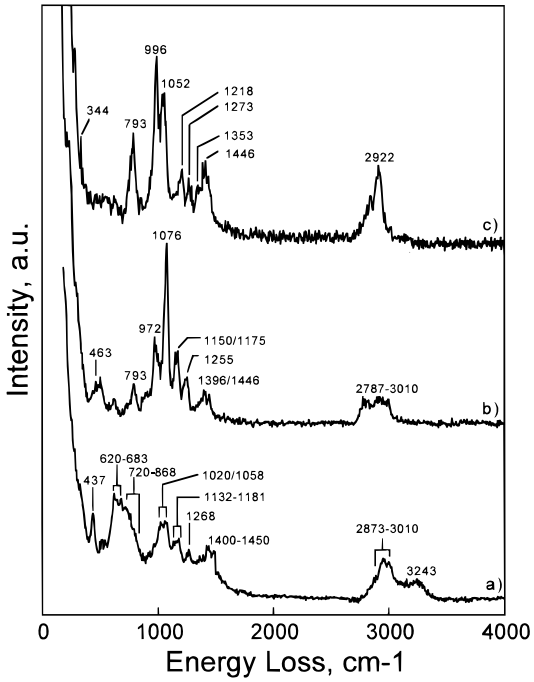

Figure 2. HREEL spectra following exposure of Ag(110) to 2-iodoethanol: (a) 15 langmuir annealed to 150 K, (b) 1.5 langmuir annealed to 230 K, and (c) 1.5 langmuir annealed to 300 K.

The major product evolved at 340 K was γ-butyrolactone (GBL), which has a stoichiometry of C_4H_6O. The lower H/C ratio for this product (1.5) with respect to the products evolved at 263 K (2.5) suggests that this pathway involves a more hydrogen-deficient intermediate. The 340 K products exhibit an overall stoichiometry of $C_2H_{3.9}O_{0.99}$, effectively C_2H_4O. We have suggested that this intermediate is an oxametallacycle species ($-CH_2CH_2O-$) that is bound to the Ag(110) surface by one carbon−silver bond and one oxygen−silver bond. Although oxametallacycle intermediates have previously been proposed in a number of different surface chemistries[14−29,39−41] they have not previously been isolated for spectroscopic characterization.

High-Resolution Electron Energy Loss Studies. High-Resolution Electron Energy Loss Spectroscopy (HREELS) experiments were conducted in order to investigate the nature of the intermediates involved in IEtOH decomposition on Ag(110). Figure 2 shows the spectra of the species present on the Ag(110) surface after briefly annealing the crystal to 150, 230, and 300 K; these spectra correspond to the intermediates present on the surface just prior to each desorption peak in Figure 1.

A comparison of the HREEL spectrum in Figure 2a with previously published liquid[42] and gas-phase[43] infrared spectra clearly shows that spectrum 2a is indicative of undissociated 2-iodoethanol multilayers. The assignment of the observed modes is described below and is summarized in Table 2.

(36) Madix, R. J.; Wachs, I. E. *Appl. Surf. Sci.* **1978**, *1*, 303.
(37) Dai, Q.; Gellman, A. *Surf. Sci.* **1991**, *257*, 103.
(38) Jones, G. S.; Barteau, M. A. unpublished results.
(39) Xu, X.; Friend, C. M. *Langmuir* **1992**, *8*, 1103.
(40) Brainard, R. L.; Madix, R. J. *Surf. Sci.* **1989**, *214*, 396.
(41) Roberts, J. T.; Madix, R. J. In *Surface Reactions*; Madix, R. J., Ed.; Springer: Berlin, 1994; p 5.
(42) Wyn-Jones, E.; Orville-Thomas, J. *J. Mol. Struct.* **1967**, *1*, 79.
(43) Homamen, L. *Spectrochim. Acta* **1983**, *39A*, 77.

Table 2. Vibrational Modes of 2-Iodoethanol and Hydroxyethyl on Ag(110), in cm^{-1}

mode[a]	multilayer ICH_2CH_2OH on Ag(110)	gas matrix ICH_2CH_2OH[42]	liquid ICH_2CH_2OH[43]	hydroxyethyl $-CH_2CH_2OH$ on Ag(110)
b(C−C−O)	326		326	
b(C−C−O)	437	431	437	463
ν(C−I)	498−541	520	516	
ν(C−I)	620−683	622	620	
$\rho(CH_2)$	720−868	751−911	795−905	793
ν(C−C)	1020	1018	977	972
ν(C−O)	1058	1073	1068	1076
δ(C−OH)	1132−1181	1111−1153	1147−1174	1150/1175
$w(CH_2)$	1268	1236/1262	1265	1255
$w,b(CH_2)$	1400−1450	1383−1469	1414−1455	1396/1446
ν(C−H)	2873−3010	2880−3032	2871−2962	2787−3010
ν(O−H)	3243	3579−3640	3360−3580	very small

[a] b = bend, ν = stretch, ρ = rock, δ = deformation, w = wag.

Although the liquid and gas-phase infrared spectra suggest the existence of modes below 300 cm^{-1}, these modes were not resolved in the present experiments. The sharp loss at 437 cm^{-1} corresponds to the bending mode of the C−C−O backbone. The broad feature in the range of 620−868 cm^{-1} can be separated into two modes. The intense modes in the range of 620−683 cm^{-1} are associated with stretching of the intact C−I bond, while the 720−868 cm^{-1} losses are assigned as rocking of the CH_2 group. The existence and intensity of the C−I stretching modes clearly suggests that the species on the Ag(110) surface at 150 K is molecular 2-iodoethanol. The doublet at 1020 and 1058 cm^{-1} is assigned to stretching of the C−C and C−O bonds, respectively. However, it may be more appropriate to think of these modes as symmetric (1020 cm^{-1}) and asymmetric (1058 cm^{-1}) C−C−O modes[37,44] due to the similarity of the C−C and C−O force constants. The losses at 1132−1181 cm^{-1} are assigned as C−OH bending modes. The assignment of this mode to δ(C−OH) is corroborated by a corresponding shift in the observed frequency for δ(C−OD) in 2-iodoethanol-d_1.[42,43] The assignment is further supported by normal coordinate calculations for both the deuterated and undeuterated derivatives.[43] The excitations in the 1400−1450 cm^{-1} range are due to various bending and wagging modes of the CH_2 group. The losses around 2873−3010 cm^{-1} are due to C−H stretching, while the broad loss at 3243 cm^{-1} is due to the O−H stretch of the intact alcohol.

The HREEL spectrum shown in Figure 2b is representative of the intermediate present on the Ag(110) surface just prior to desorption of the C_2 products evolved at 263 K and has been identified as a hydroxyethyl species. This assignment is entirely consistent with the deductions made previously from the TPD data. The individual mode assignments are summarized in Table 2 and are made by comparison of spectrum 2b with infrared spectra for 2-iodoethanol found in the literature.[42,43] The similarity between the HREEL spectrum for hydroxyethyl and that for 2-iodoethanol is not surprising: both species can be characterized as low-mass ligands bound to a massive atom (iodine) or surface. The key distinguishing feature of the hydroxyethyl spectrum, compared to the 2-iodoethanol spectrum, is the strong intensity decrease of the C−I stretching mode—the broad loss at 620−680 cm^{-1} which was the most intense peak in spectrum 2a. The weak loss remaining at 615 cm^{-1} in spectrum 2b is most likely due to trace amounts of 2-iodoethanol either remaining on the surface or possibly readsorbed from the chamber background after heating the surface to 230 K. Although the C−I bond was obviously broken at this temperature, we were unable to resolve the stretching modes associated with the Ag−C bond or Ag−I bonds which would be formed as a consequence. Based upon the corresponding Ag−C stretching mode for ethyl−Ag(110), the Ag−C mode would be expected around 330−340 cm^{-1}.[45] Although this mode was not resolved, there is evidence that the hydroxyethyl is bound to the surface via a Ag−C bond. Often, surface species with CH_2 groups bound directly to metal atoms exhibit $\nu(CH_2)$ modes which are significantly redshifted or softened with respect to their normal frequencies.[46,47] The broad feature at 2787−3010 cm^{-1} in spectrum 2b is consistent with contributions from both normal and softened $\nu(CH_2)$ modes, indicating that some of the C−H stretching modes are due to CH_2 groups bound directly to the silver surface. The fact that the hydroxyl function remains intact at 230 K serves as further evidence for the hydroxyethyl intermediate. This assertion is based upon the persistence of the δ(C−OH) mode which remains at 1150−1175 cm^{-1}. The O−H stretching mode present at 3243 cm^{-1} from the 2-iodoethanol multilayer spectrum (Figure 2a) was not readily observed for the hydroxyethyl; however, this mode was not detected for hydroxyethyl or monolayer 2-iodoethanol on Rh(111) either. On Rh(111) it was also necessary to use the δ(C−OH) mode to fingerprint intact OH groups in these adsorbates.[27] The frequency of 972 cm^{-1} for the C−C stretching mode was redshifted by ≈50 cm^{-1} with respect to intact 2-iodoethanol. The C−O stretch at 1076 cm^{-1} was by far the most intense loss in the hydroxyethyl spectrum. The excitations at 1255, 1396, and 1446 cm^{-1} correspond to various CH_2 modes while the losses at 2787−3010 cm^{-1} are indicative of C−H stretches.

The TPD analysis of the 263 K intermediate indicated that the stoichiometry of this intermediate is C_2H_5O, which is consistent with either a hydroxyethyl or an ethoxide intermediate. To further substantiate the case for the hydroxyethyl, a separate set of experiments was performed in which an ethoxide was spectroscopically characterized. The ethoxide was formed by exposing an oxygen-precovered Ag(110) surface to ethanol followed by annealing the surface to 230 K. For comparison, the HREEL spectrum of ethoxide is compared to the hydroxyethyl spectrum in Figure 3. The ethoxide spectrum shown in Figure 3a is virtually identical to previously published ethoxide results,[37] but is quite distinct from the hydroxyethyl spectrum. The mode assignments for the ethoxide and hydroxyethyl are compared in Table 3 and the major differences are described below. The most obvious difference between the vibrational spectrum of an ethoxide (Figure 3a) as compared to that of a hydroxyethyl (Figure 3b) is the dramatic difference in the frequency associated with stretching of the C−C bond. The C−C stretching mode for the ethoxide has a frequency of 880 cm^{-1} while the same mode for the hydroxyethyl is located at 972 cm^{-1}. This divergence is not surprising considering that the hydroxyethyl is bound to the Ag(110) surface by an Ag−C bond while the ethoxy is anchored by an Ag−O bond. The other key distinguishing feature between the two spectra is the presence (hydroxyethyl) or absence (ethoxide) of the C−OH deformation mode located at 1150/1175 cm^{-1} for the hydroxyethyl intermediate. Also, the hydroxyethyl is distinguished by its softened $\nu(CH_2)$ modes which are not present for the ethoxide species. Again, this difference is expected on the basis of the structures of the two species. In addition, the CH_2 rocking mode detected at 793 cm^{-1} for the hydroxyethyl was not present in the ethoxide spectrum. The remaining modes were qualitatively

(44) Davis, J. L.; Barteau, M. A. *Surf. Sci.* **1990**, *235*, 248.
(45) Jones, G. S.; Barteau, M. A.; Vohs, J. M. unpublished results.
(46) Li, J. L.; Bent, B. E. *Chem. Phys. Lett.* **1992**, *194*, 208.
(47) Lee, M. B.; Yang, Q. Y.; Tang, S. L.; Ceyer, S. T. *J. Chem. Phys.* **1996**, *85*, 1693.

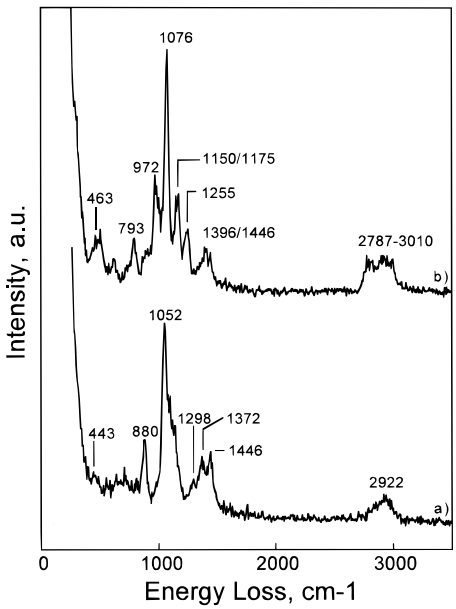

Figure 3. Comparison of the HREEL spectra for (a) ethoxide and (b) hydroxyethyl. The ethoxide spectrum was collected after dosing the oxygen-covered Ag(110) surface with ethanol and annealing to 230 K.

Table 3. Vibrational Modes of C_2H_5O Intermediates, Ethoxide and Hydroxyethyl, on Ag(110), in cm^{-1}

mode[a]	ethoxide $-OCH_2CH_3$ on Ag(110)[b]	ethoxide $-OCH_2CH_3$ on Ag(110)[37]	hydroxyethyl $-CH_2CH_2OH$ on Ag(110)
ν(Ag−O)	n.r.	270	
b(C−C−O)	443	475	463
$\rho(CH_2)$			793
ν(C−C)	880	890	972
ν(C−O)	1052	1060	1076
δ(C−OH)			1150/1175
w(CH_2)	1298	1290	1255
$\delta(CH_2), \delta(CH_3)$	1372	1370	
	1446	≈1450	
w,b(CH_2)			1396/1446
ν(C−H)	2922	2915	2787−3010
ν(O−H)			very small

[a] ν = stretch, b = bend, ρ = rock, δ = deformation, w = wag. [b] This work.

similar, including the most intense mode which was due to the C−O stretch of both species.

The vibrational spectrum of the species present on the Ag(110) surface after annealing to 300 K is shown in Figure 2c. Distinct changes in the vibrational spectrum occurred as a result of annealing the Ag(110) surface to 300 K. In particular, the 793 and 996 cm^{-1} modes dramatically increased, with the 996 cm^{-1} mode becoming the most intense. Also, the δ(C−OH) mode present at 1150/1175 cm^{-1} in Figure 2b is missing in Figure 2c. The spectrum is representative of the intermediate responsible for the evolution of γ-butyrolactone and other products at 340 K. The assignment of the experimentally observed vibrational modes is based upon a comparison with the modes for an oxametallacycle predicted by using Density Functional Theory (DFT) and is discussed in the following section.

Comparison of Experimental HREEL Spectrum and Theoretical IR Spectrum. The HREEL spectrum shown in Figure 2c is representative of an oxametallacycle and its modes have been assigned by comparison to the theoretical IR spectrum calculated for an oxametallacycle incorporating two silver atoms

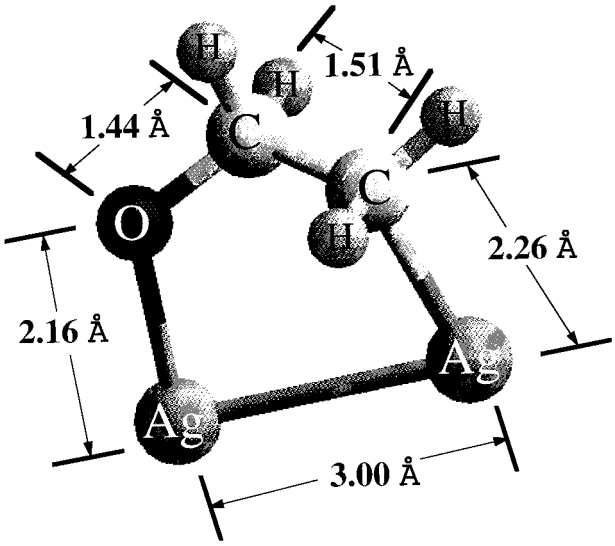

Figure 4. Fully optimized structure for an oxametallacycle adsorbed onto a 2-atom silver cluster. The final nonplanar structure was predicted by using DFT calculations.

by using Density Functional Theory (DFT). The oxametallacycle structure for which the IR spectrum was calculated was previously fully optimized via a total energy minimization technique and the optimized structure is illustrated in Figure 4. The calculated bond lengths for this structure have physically realistic values and are also shown in Figure 4. The mode assignments for the experimentally obtained HREEL spectrum were based on a direct comparison with the theoretical IR spectrum of the oxametallacycle, through a comprehensive animation of the calculated vibrational modes.

The theoretical IR spectrum and the experimental HREEL spectrum are shown in Figure 5 along with the corresponding mode assignments. There is an obvious and direct agreement between the calculated spectrum and that observed experimentally. In fact, the frequencies of all of the major modes observed in the HREEL spectrum match the predicted frequencies to within 5%. The main emphasis should be placed on comparing the frequencies of the modes rather than the intensities. It may be misleading to compare relative intensities since the dipole-scattering selection rules which affect the intensity of losses observed in HREELS experiments are not captured in the theoretical spectrum.

A comparison of the calculated and experimental modes is given in Table 4 and is discussed below. The predicted infrared frequencies in Table 4 have been multiplied by a scaling factor of 1.02 in order to align the most intense predicted C−H stretch with the most intense experimentally observed C−H stretch. Also, in Table 4 and in the following discussion, the two carbons of the oxametallacycle will be distinguished as C^1 and C^2, where C^1 represents the bridging carbon which is bonded to the oxygen and C^2 is the carbon bound to the silver surface (i.e., $-O-C^1-C^2-$). Finally, the following discussion will treat the experimental spectrum and compare it to the calculated spectrum, rather than vice-versa. The loss resolved as a shoulder at 344 cm^{-1} matches the calculated excitation at 366 cm^{-1} and is identified as the in-phase stretching of the Ag−O and Ag−C^2 bonds. The most intense features of the oxametallacycle vibrational spectrum are classified as O−C^1−C^2 deformations and occur in the 793−1052 cm^{-1} frequency range. The intense loss at 793 cm^{-1} corresponds to the predicted loss at 825 cm^{-1} and is assigned to the symmetric stretching of the O−C^1−C^2 backbone. This mode can be thought of as the in-phase

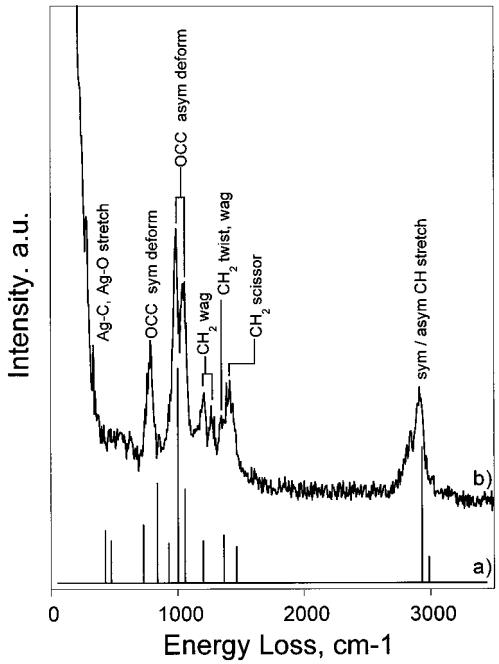

Figure 5. Comparison of the vibrational spectra (a) calculated and (b) experimentally observed for an oxametallacycle adsorbed onto silver. The infrared spectrum shown in (a) was predicted by using DFT calculations for the oxametallacycle structure shown in Figure 4. The HREEL spectrum shown in (b) was collected experimentally. The mode assignments are based upon motions observed for the vibrational animations of the fully optimized structure calculated by DFT, shown in Figure 4.

Table 4. Vibrational Modes of Oxametallacycle Adsorbed on Ag(110) versus Those Predicted by DFT Calculations, in cm^{-1}

mode[a]	exptl $-OC^1H_2C^2H_2-$ on Ag(110)	theoretical (DFT) $-OC^1H_2C^2H_2-$ on Ag dimer
ν_s(Ag−O),(Ag−C^2)	344	366
ν_a(Ag−O),(Ag−C^2)		405
δ(O−C^1−C^2)		455
tw (C^2H_2)		717
ν_s(O−C^1−C^2)	793	825
τ(C^1−C^2)		905
ν_a(O−C^1−C^2)	996	997
ν_a(O−C^1−C^2)	1052	1024
tw(C^1H_2)	1218	1192
w(CH_2)	1273	
w(C^1H_2), tw(C^2H_2)	1353	1357
out of phase χ(CH_2)	1446	1451
in phase χ(CH_2)	1446	1453
ν_a(C^1−H)	2922	2923
ν_s(C^2−H)	2922	2990

[a] ν_s = symmetric stretch, ν_a = asymmetric stretch, δ = deformation, tw = twist, τ = torsion, w = wag, b = bend, χ = scissor.

stretching of the O−C^1 and C^1−C^2 bonds. The doublet observed at 996 and 1052 cm^{-1} in the HREEL spectrum is accurately predicted by theory at frequencies of 997 and 1024 cm^{-1}. Both of these modes represent the asymmetric or out-of-phase stretching of the O−C^1−C^2 unit. The excitations observed in the 1200−1450 cm^{-1} frequency range correspond to the various motions of the CH_2 groups. The CH_2 modes in this region are coupled, making description of the vibrations somewhat laborious. The motions characterized below account for the main vibrations for each observed loss. The loss observed at 1218 cm^{-1} agrees with the calculated loss at 1192 cm^{-1}. The molecular motion associated with this feature is best described as twisting of the C^1H_2 group in the O−C^1−C^2 plane. The feature detected at 1273 cm^{-1} does not directly match any of the predicted losses well but likely represents a CH_2 motion as well. The excitation located at 1353 cm^{-1} closely matches that at 1357 cm^{-1} predicted by theory. This mode is characterized as an in-plane C^1H_2 wag coupled with a C^2H_2 twist. The final CH_2 mode at 1446 cm^{-1} matches both the 1451 and 1453 cm^{-1} predicted frequencies and corresponds to both the in-phase and out-of-phase scissor modes of both CH_2 groups. The remaining broad loss centered at 2922 cm^{-1} is in accord with the predicted losses at 2923 and 2990 cm^{-1} corresponding to the asymmetric and symmetric C−H stretches, respectively. As with the hydroxyethyl species, the skewing of this peak to lower frequencies provides evidence for softening of the $\nu(CH_2)$ modes, indicating that a CH_2 group, corresponding to C^2, is bound to the silver surface.

Discussion

Until now investigations that have proposed oxametallacycles as surface species have relied upon circumstantial evidence, principally from TPD data.[14−29,40,41] Although many of these studies make a thorough case for oxametallacycles based upon indirect evidence, they have been met with some skepticism due to the lack of spectroscopic evidence. The situation is similar for these ligands in the organometallic literature where they have been the subject of questions such as "Metallaoxetanes—Reality or Fiction?"[5] While there is spectroscopic evidence for matrix-isolated metallaoxetanes[8,9] we believe that the current study represents the first investigation to provide concrete spectroscopic evidence for surface oxametallacycles. The following discussion focuses on (1) the characteristics of oxametallacycles which make them difficult to isolate, (2) the reasons why the current approach was successful, (3) the DFT calculations necessary for conclusive identification of the oxametallacycle, and (4) the observed reactivity of oxametallacycles on silver surfaces.

This study is the first investigation in which a stable oxametallacycle has been isolated and/or spectroscopically characterized on any transition metal surface. With that in mind it is worth considering the characteristics which make this intermediate so difficult to isolate. This difficulty stems in part from the fact that it contains a bidentate, asymmetric ligand. Examples of stable symmetric analogues of oxametallacycles can be found in the surface science literature. Madix and coworkers have shown that the formation and characterization of dialkoxides such as 1,2-ethanedioxy and 1,2-propanedioxy can be readily achieved by reaction of the corresponding diols on oxygen-dosed Ag(110).[48−51] In addition, Lambert and coworkers have proposed hydrocarbon metallacycles as intermediates in the cyclotrimerization of acetylene to form benzene on Pd(111). These intermediates are metallacyclopentadiene complexes which are formed by the linking of two acetylene molecules.[52−57] The above examples are distinguished from oxametallacycles in that the ligands are bound to the respective

(48) Capote, A. J.; Madix, R. J. *Surf. Sci.* **1989**, *214*, 276.
(49) Capote, A. J.; Madix, R. J. *J. Am. Chem. Soc.* **1989**, *111*, 3570.
(50) Ayre, C. R.; Madix, R. *J. Surf. Sci.* **1993**, *303*, 279.
(51) Ayre, C. R.; Madix, R. *J. Surf. Sci.* **1993**, *303*, 297.
(52) Tysoe, W. T.; Lambert, R. M.; Nyberg, G. L. *Surf. Sci.* **1983**, *135*, 128.
(53) Patterson, C. H.; Lambert, R. M. *J. Am. Chem. Soc.* **1988**, *110*, 6871.
(54) Patterson, C. H.; Timbrell, P. Y.; Mundenar, J. M.; Gellman, A. J.; Lambert, R. M. *Surf. Sci.* **1989**, *208*, 93.
(55) Ormerod, R. M.; Lambert, R. M. *Surf. Sci.* **1990**, *225*, L20.
(56) Ormerod, R. M.; Lambert, R. M. *J. Phys. Chem.* **1992**, *96*, 8111.
(57) Pacchioni, G.; Lambert, R. M. *Surf. Sci.* **1994**, *304*, 208.

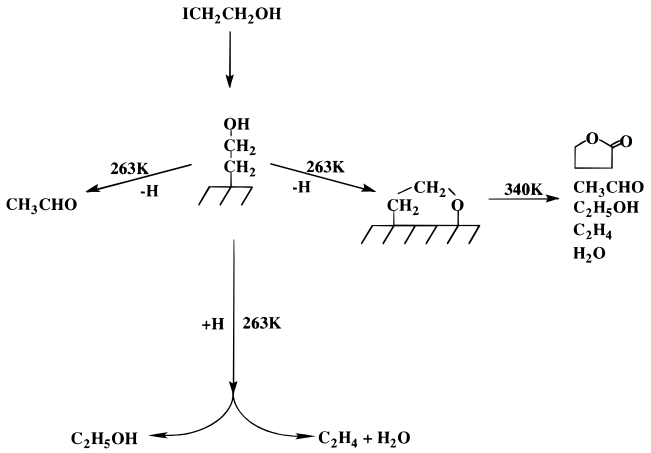

Figure 6. Overall reaction scheme for the decomposition of 2-iodoethanol on Ag(110).

surfaces by equivalent chemical functions at each end. Oxametallacycles on the other hand are bound to the surface by one carbon−metal bond and one oxygen−metal bond. Formation of oxametallacycles under conditions where they are thermally stable therefore presents a greater synthetic challenge; one must activate dissimilar chemical functions without inducing further reaction or decomposition.

Insight as to why the 2-iodoethanol chemistry led to the formation of a stable surface oxametallacycle can be gained by comparing that chemistry with other reactions which have been proposed to take place via oxametallacycles on silver surfaces. The only example of that type is the reaction of tertiary butanol on oxygen-covered Ag(110), which Brainard and Madix have proposed to take place via an oxametallacycle intermediate. A comparison between the 2-iodoethanol and *tert*-butyl alcohol chemistries suggests that the sequence in which and the method by which the Ag−C and Ag−O bonds of the oxametallacycle are formed apparently have a great influence on the likelihood that a stable oxametallacycle will be formed. The reactions of *tert*-butyl alcohol on oxygen-covered Ag(110) take advantage of the fact that surface oxygen will abstract the hydroxyl proton thus forming *tert*-butoxide. This reaction occurs below 200 K and is responsible for Ag−O bond formation. The remaining step for oxametallacycle formation then would involve cleavage of a methyl C−H bond and formation of the Ag−C bond. However, for *tert*-butoxide the electronegative oxygen atom is not adjacent to the methyl carbon so that the homolytic dehydrogenation of that carbon is not facilitated. In fact, under oxygen-lean conditions the methyl C−H bond of the *tert*-butoxide intermediate is not broken until 510 K on silver, a temperature at which the oxametallacycle is not stable.[21,22,41]

For comparison, the basic steps involved in the reaction of 2-iodoethanol on Ag(110) are summarized in Figure 6 along with the ultimate products. In the present study we have taken advantage of the relative weakness of the carbon−iodine bond of 2-iodoethanol in order to form a species initially bound to the surface by a Ag−C bond, the hydroxyethyl. The simplest step for oxametallacycle formation then would be activation of the hydroxyl function to form the Ag−O bond. This synthesis route is essentially the reverse of that suggested by Day et al., who formed a hydroxyalkyl from an iridaoxetane in solution.[58] Oxygen-free silver surfaces do not typically activate organic alcohols prior to alcohol desorption from the surface.[36] However, the hydroxyethyl formed from 2-iodoethanol is bound by its Ag−C bond and therefore remains on the surface until it undergoes decomposition at 263 K. The details of this decomposition process remain unclear. One reaction channel that cannot be ruled out is β-hydride elimination to form vinyl alcohol. Rapid rearrangement of this species could lead to one or more of the observed products, acetaldehyde and oxametallacycles. However, the simplest route to the oxametallacycle is sequential scission of the C−I and O−H bonds of iodoethanol. In any case, the formation of the oxametallacycle occurs at a temperature, 263 K, where this intermediate is stable. Note that this temperature is approximately 250 K less than that for the proposed oxametallacycle formation step in the *tert*-butyl alcohol example. The reaction of 2-iodoethanol was initiated by the formation of the Ag−C bond of the metallacycle at low temperatures by breaking the C−I bond in 2-iodoethanol, thereby circumventing the energy intensive C−H bond cleavage step which prevented formation of a stable oxametallacycle in the *tert*-butyl alcohol chemistry.

Since examples of other stable surface oxametallacycles are nonexistent, we must obtain spectroscopic standards from other sources. Density Functional Theory has recently emerged as an accurate tool for predicting chemical structures, vibrational frequencies, and other physical/chemical properties of various species (molecules, ions, radicals, intermediates). DFT calculations which incorporate nonlocal gradient corrections for correlation and exchange can be expected to give bond lengths to within 0.01−0.05 Å, bond angles to within 1−2°, bond energies to within 2 kcal/mol, and Raman and infrared frequencies to within 5% of experimental values for transition metal containing systems.[59] The vibrational frequencies of a variety of simple adsorbates on different metal clusters have been accurately predicted recently by using DFT methods.[60−74] As the level of computational resources increases, so does the size of the systems accessible for computational studies. Neurock and co-workers have recently performed frequency calculations for maleic anhydride adsorbed through either di-σ or π interactions onto Pd(111) clusters. The predicted vibrational frequencies for maleic anhydride match the experimental HREELS data of Xu and Goodman to within 5%.[75,76]

We have used DFT calculations to aid in the assignment of the experimentally obtained HREEL spectrum for an oxamet-

(58) Day, V. W.; Locklegde, S. P.; Klemperer, W. G.; Main, D. J. *J. Am. Chem. Soc.* **1990**, *112*, 2031.

(59) van Santen, R. A.; Neurock, M. *Catal. Rev.-Sci. Eng.* **1995**, *37*, 557.

(60) Mijoule, C.; Salahub, D. R.; Bouteiller, Y. *Surf. Sci.* **1991**, *253*, 375.

(61) Rochefort, A.; Salahub, D. R.; McBreen, P. H. *Surf. Sci.* **1996**, *347*, 11.

(62) Papai, I.; Salahub, D. R. *Surf. Sci.* **1993**, *282*, 262.

(63) Baba, M. F.; Godbout, N.; Mijoule, C.; Salahub, D. R. *Surf. Sci.* **1994**, *316*, 349.

(64) Yang, D. S.; Berces, A.; Zgierski, M. Z.; Hacket, P. A.; Roy, P. N.; Martinez, A.; Carrington, T., Jr.; Salahub, D. R.; Fournier, R.; Pang, T.; Cheng, C. *J. Chem. Phys.* **1996**, *105*, 10663.

(65) Ushio, J.; St. Amant, A.; Papai, I.; Salahub, D. R. *Surf. Sci. Lett.* **1992**, *262*, L134.

(66) Martinez, A.; Salahub, D. R.; Koster, A. M. *J. Phys. Chem.* **1997**, *101*, 1532.

(67) Chertihin, G. V.; Neurock, M.; Andrews, L. *J. Phys. Chem.* **1996**, *100*, 14609.

(68) Chertihin, G. V.; Yustein, J. T.; Saffel, W.; Andrews, L.; Neurock, M.; Ricca, A.; Bauschlicher; C. W., Jr. *J. Phys. Chem.* **1996**, *100*, 5261.

(69) Andrews, L.; Brabson, G. D.; Hassanzadeh, P.; Citra, A.; Neurock, M. *J. Phys. Chem.* **1996**, *100*, 8273.

(70) Jigato, M. P.; Somasundram, V. T. K.; Handy, N. C.; King, D. A. *Surf. Sci.* **1997**, *380*, 83.

(71) Jonas, V.; Thiel, W. *J. Chem. Phys.* **1996**, *105*, 3636.

(72) van Daelen, M. A.; Newsam, J. M.; Li, Y. S.; van Santen, R. A. *J. Phys. Chem.* **1996**, *100*, 2279.

(73) Ball, D. W.; Chiarelli, J. A. *J. Mol. Struct.* **1995**, *372*, 113.

(74) Ruschel, G. K.; Nemetz, T. M.; Ball, D. W. *J. Mol. Struct.* **1996**, *384*, 101.

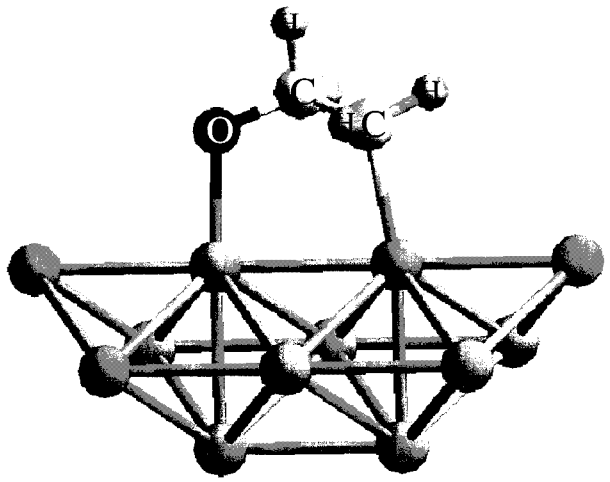

Figure 7. Geometrically optimized structure for an oxametallacycle adsorbed onto a 12-atom silver cluster representing the Ag(110) surface. The structure was optimized by using DFT calculations.

allacycle adsorbed on the Ag(110) surface. All of the main modes observed experimentally compare to the theoretically predicted frequencies to within 5%. In particular, the DFT calculations accurately predict the main spectral features which are due to the OCC stretches, including the doublet at ≈1000 cm^{-1}. Although the relative intensities of the theoretical spectral features approximately match those of the HREEL spectrum, this is somewhat fortuitous as the theoretical predictions do not account for the dipole scattering selection rules in HREELS on metal surfaces.[77] In addition to predicting the observed frequencies, the sometimes complicated molecular motions associated with the various modes were animated as well, allowing for clear identification of individual modes. The power of quantum chemistry, within the framework of DFT, becomes quite evident here, where in the absence of any prior spectroscopic information we are still able to conclusively identify the surface intermediate as an oxametallacycle.

To test the accuracy of the 2-silver-atom cluster calculations, subsequent geometry optimization and frequency calculations for an oxametallacycle adsorbed onto a 12-silver-atom cluster were performed. That 12-silver-atom cluster with the optimized adsorbed oxametallacycle is shown in Figure 7 and is meant to represent the ridge of the ideal Ag(110) surface. The optimized structure for the oxametallacycle adsorbed onto a 12-silver-atom cluster is obviously quite similar to that for the oxametallacycle adsorbed onto a silver dimer. The infrared vibrational frequencies calculated for oxametallacycles bound to a silver dimer and to a 12-silver-atom cluster are listed in Table 5, for direct comparison. Two sets of frequency calculations were performed for the oxametallacycle adsorbed on the 12-silver-atom cluster: (1) only C, H, and O atoms were displaced from their optimal positions to calculate frequencies, whereas Ag atoms were kept fixed ("fixed-cluster" frequency calculations), and (2) all atoms, including Ag, C, H, and O, were displaced during frequency calculations ("nonfixed-cluster" frequency calculations). There are several key points to be made regarding these frequency calculations. The first and most important observation is that the frequencies calculated are nearly independent of cluster size. The close correlation between the predicted

Table 5. Comparison of Cluster Size Effect on DFT Predicted Infrared Vibrational Frequencies for Oxametallacycle

2-silver-atom nonfixed cluster (cm^{-1})	12-silver-atom fixed cluster (cm^{-1})	12-silver-atom nonfixed cluster (cm^{-1})
250	236	243
366	333	354
405	365	393
455	452	455
717	654	654
825	824	825
905	901	902
997	987	987
1024	1027	1027
1128	1129	1130
1192	1191	1191
1357	1344	1344
1451	1452	1451
1454	1463	1462
2807	2803	2803
2923	2923	2923
2990	3013	3013
3102	3108	3108

frequencies for the silver dimer and 12-atom cluster, as well as the experimental frequencies, demonstrates that the computationally less expensive silver dimer calculations do a more than adequate job in capturing the physics of the oxametallacycle and its molecular motions. Another important observation is that all of the predicted modes with frequencies above 200 cm^{-1} are due to motion of the organic ligand and involve very little motion of the substrate silver atoms. In fact no silver atom motion was detected in the DFT animation for modes with frequencies above 400 cm^{-1}. This observation explains why the predicted frequencies for the 12-atom "fixed" cluster and 12-atom "nonfixed" cluster are nearly identical above 400 cm^{-1}. The only difference between the predicted vibrational spectrum for the 12-atom "fixed" cluster and 12-atom "nonfixed" cluster is that the spectrum for the "nonfixed" cluster has many modes with frequencies below 200 cm^{-1} associated with motion of the silver atoms (metal phonon modes). These low-frequency modes are dominated by deformations of the silver cluster; the accompanying motions of the organic ligand appear to be driven by the need to maintain coordination to the moving metal atoms beneath. The fact that all of the predicted modes with frequencies in the experimentally observable frequency range are due to motions of the organic ligand may help to explain why the simple silver dimer oxametallacycle calculations do such a good job of predicting the experimentally observed modes.

Finally, it is appropriate at this point to comment briefly on the reactivity of oxametallacycles. Although no ethylene oxide was formed from the oxametallacycle in the 2-iodoethanol chemistry presented here, there seems to be an inherent link between oxametallacycle intermediates and epoxides. Oxametallacycles or metallaoxetanes have been implicated in the ring opening of epoxides on Pd(110),[14] Pd(111),[15] and Rh(111)[16] surfaces; matrix-isolated Fe[8] and Ni[9] species; and Pt, Cu, V, W, Mo, Ni, and Ir organometallic complexes in solution.[7] In addition, oxametallacycles have been proposed to be involved in the formation of epoxides on the Ag(110) surface,[21,22,41] as well as the formation of epoxides from Cr, Pt, Ni, and Pd organometallic complexes in solution.[7] Given these suggested connections between oxametallacycles and epoxides and the fact that silver is an industrially used epoxidation catalyst, the question arises as to how stable oxametallacycles on silver might be converted to ethylene oxide.

(75) Neurock, M.; Venkataraman, P. S.; Coulston, G. W. Proceedings of 15th Meeting of the North American Catalysis Society; Chicago, IL, 1997.

(76) Xu, C.; Goodman, D. W. *Langmuir* **1996**, *12*, 1807.

(77) Ibach, H. *Electron Energy Loss Spectroscopy and Surface Vibrations*; Academic Press Inc.: New York, 1982.

The question of ethylene oxide formation can be addressed in the following way. To form γ-butyrolactone from two oxametallacycles the bridging-carbon (C^1) on one of the oxametallacycles must lose both of its hydrogens. This dehydrogenation is effectively a β-hydride elimination, whichever end of the ligand one counts from. Recalling that the oxametallacycle derived from *tert*-butyl alcohol proposed by Brainard and Madix had no such bridging-carbon hydrogens (only methyls) may help to explain the difference in product slates. The oxametallacycle in that case was formed (and decomposed) at 510 K, a temperature apparently insufficient to induce $C-CH_3$ scission. Ring closure to form the epoxide, isobutylene oxide, and C−O scission to form isobutylene were alternate reaction pathways which were energetically favorable at this temperature. This reasoning would suggest that ethylene oxide was not formed in the current study because it was precluded by the dehydrogenation of the oxametallacycle, leading to the formation of γ-butyrolactone, among other products, at lower temperatures. However, the industrially used ethylene epoxidation catalyst (Ag/Al_2O_3) includes many promoters such as Cs, Cl, and subsurface oxygen which were not present on our model Ag(110) catalyst.[78] Of particular importance is the fact that Cs has been reported to lower the desorption energy of epoxides from silver surfaces.[2] The inclusion of Cs and other promoters in future studies may serve to facilitate the formation of ethylene oxide by making this reaction pathway more energetically competitive with γ-butyrolactone formation. In fact, a possible reaction coordinate for ring closure to form ethylene oxide was observed in the DFT animation of the calculated vibrations for the oxametallacycle. The vibrational mode predicted at 717 cm^{-1} for the silver-dimer oxametallacycle represents a vibrational motion where the terminal oxygen and carbon atoms of the oxametallacycle approach each other in a motion which resembles that expected for ring closure to form ethylene oxide. We suggest that this is the reaction coordinate for ethylene oxide formation since it is the only mode where the terminal oxygen and carbon approach each other without twisting of the terminal CH_2 to place a hydrogen atom in a position blocking C−O bond formation.

(78) Hucknall, D. J. *Selective Oxidation of Hydrocarbons*; Academic Press Inc.: London, 1974.

Conclusions

2-Iodoethanol decomposes via sequential hydroxyethyl and oxametallacycle intermediates on Ag(110). Both of these species were isolated cleanly for the first time on a metal surface and spectroscopically characterized by using HREELS. A comparison of the experimental HREEL spectrum with the DFT-calculated infrared spectrum for an oxametallacycle unequivocally identifies that intermediate as well as its vibrational motions. The identification of the oxametallacycle is consistently supported by DFT calculations regardless of the size of the cluster used. The stable oxametallacycles isolated here demonstrated a new reaction pathway not previously attributed to them. Under the conditions of this study oxametallacycles couple to form γ-butyrolactone rather than undergoing unimolecular cyclization to form ethylene oxide as might be expected. However, a possible reaction coordinate for the conversion of an oxametallacycle to ethylene oxide was identified from the DFT-calculated molecular vibrations of the oxametallacycle. Future studies may elucidate the role of promoters in converting an oxametallacycle to ethylene oxide.

Acknowledgment. The authors gratefully acknowledge the financial support (Grant FG02-84ER13290) for this research by the U.S. Department of Energy, Office of Basic Sciences, Division of Chemical Sciences. G.S.J. would like to thank the DuPont Company for financial assistance in the form of a graduate fellowship. Finally, the assistance of Dr. Russell Plank in collecting the HREEL spectra was greatly appreciated.

JA973609H